RSC Advances

PAPER

View Article Online
View Journal | View Issue

Cite this: *RSC Adv.*, 2026, **16**, 16241

Seven new octapeptides from the mangrove rhizosphere-derived *Streptomyces* sp. GXIMD 03507

Yanan Wang, Rongchun Qin, Zhenzhou Tang, Mi Zhou, Peiying Xue, Chunxiao Chen, Jingqi Zhu, Yongxue Du, Xiaodong Jiang,* Yonghong Liu * and Xiao Lin *

Received 16th December 2025
Accepted 17th March 2026

DOI: 10.1039/d5ra09728b

rsc.li/rsc-advances

Mangrove-derived actinomycetes are a rich reservoir of bioactive natural products, offering promising opportunities for new lead discovery. Seven new quinomycin-type octapeptides, designated quinomycin Q–U and triostin D–E, were isolated from the mangrove rhizosphere-derived *Streptomyces* sp. GXIMD 03507. The structures of compounds **1–7**, including their absolute configurations were elucidated through a combination of chemical and spectroscopic analyses. The anti-proliferation activities of compounds **1–7** were evaluated against five tumor cell lines. None of the compounds (**1–7**) exhibited significant cytotoxic activity. These results suggested that the bicyclic framework bridged by ester linkages is crucial for biological activity, hydrolysis of one or both of these ester bonds dramatically decreases the cytotoxic potency.

Introduction

Recently, drug resistance and pathogen mutations have weakened the effectiveness of many anticancer and antimicrobial drugs. This challenge underscores the urgent need to discover new chemotypes and pharmaceutical resources. Mangrove ecosystems, widely distributed across tropical and subtropical intertidal zones, are promising environments for such discovery. Mangrove plants, have adapted to harsh environments, including high salinity and tidal flooding, supporting diverse microbial community in the rhizosphere soil.[1] Many of these microbes produce structurally diverse metabolites with distinct biological functions, and mangrove-derived microorganisms have emerged as a rich source of new drug leads.[2,3]

Within these communities, *Streptomyces* species are prolific members of mangrove-associated microbiota and are renowned for producing structurally complex natural products.[4] Numerous studies have shown that secondary metabolites isolated from *Streptomyces* sp. exhibit potential as new antibiotics, antitumor agents, immunosuppressive agents and enzyme inhibitors.[5] Among these metabolites, quinomycins constitute a family of octapeptides characterized by two aromatic heterocycles tethered to a dimerized peptide core and act as DNA bisintercalators. To date, approximately 40 quinomycins have been reported from various *Streptomyces* sp.[6]

In our ongoing efforts to explore bioactive marine peptides from microorganisms, we discovered that the fermentation extract of strain GXIMD 03507 contained quinomycin-type peptides. This strain was isolated from mangrove rhizosphere soil in Dongxing, Guangxi, China, and was identified as *Streptomyces* sp. Liquid chromatography-photodiode array-mass spectrometry (LC-PDA-MS) analysis of the culture extract revealed several previously undescribed quasi-molecular ions with UV absorption profiles closely resembling that of echinomycin (Fig. S2), suggesting the presence of new quinomycin-type metabolites. Inspired by these findings, we expanded our chemical exploration of this strain, leading to the discovery of seven new quinomycin-type octapeptides, designated as quinomycins Q–U (**1–5**) and triostins D–E (**6–7**), along with four known compounds quinomycin G (**8**),[7] depsiechinoserine (**9**),[8] echinoserine (**10**),[9] and echinomycin (**11**).[10] Herein, we describe the isolation, structural elucidation, and cytotoxic evaluation of **1–7**, which expand the chemical diversity of the quinomycin family and under core mangrove-derived *Streptomyces* as a valuable reservoir of drug leads.

Results and discussion

Liquid chromatography-mass spectrometry (LC-PDA-MS) analysis was performed on quinomycin-type octapeptide subfractions extracted from the liquid medium of *Streptomyces* sp. GXIMD 03507, and revealed the presence of undescribed MS profile with $[M + H]^+$ ions ranging from m/z 1101 to 1123 (Fig. S2). Large-scale fermentation was conducted to produce the target compounds, followed by extensive combinatorial

Guangxi Key Laboratory of Marine Drugs, University Engineering Research Center of High-efficient Utilization of Marine Traditional Chinese Medicine Resources, Institute of Marine Drugs, Guangxi University of Chinese Medicine, Guangxi, China. E-mail: linxiaolegend@163.com

chromatographic purification, which ultimately yielded seven new quinomycin-type octapeptides (compounds **1–7**).

Quinomycin Q (**1**) was obtained as a white amorphous powder. Its molecular formula was deduced as $C_{51}H_{64}N_{12}O_{12}S_2$ by HRESI-MS measurement (*m/z* 1101.4288 $[M + H]^+$, calcd for $C_{51}H_{65}N_{12}O_{12}S_2$, 1101.4286 $[M + H]^+$), indicating 26 degrees of unsaturation (attributes to aromatic rings, carbonyl groups, and olefinic groups). The UV spectrum showed maximum absorption bands at 201, 242, 318, and 324 nm (Fig. S3), suggesting the presence of a quinoxaline-2-carboxylic acid chromophore.[7,11]

The ^{1}H NMR data (Table 1) of **1** displayed four NH protons (δ_H 7.38, 7.51, 10.56, and 10.58), the characteristic signals (δ_H 7.90–7.81, 8.23–8.14) of two quinoxaline-2-carboxylic acids (QXA and QXA′), four *N*-methyl groups (δ_H 3.02–3.07) and a *S*-methyl group (δ_H 2.06). The ^{13}C NMR spectra (Table 1), with the assistance of 2D NMR, revealed the presence of 51 carbons signals, including eight carbonyls (δ_C 173.1, 172.6, 170.7, 170.7, 169.4, 169.4, 163.3, 162.9), two quinoxaline-2-carboxylic acid moiety carbons (δ_C 162.2, 162.2, 129.6–144.1), two olefinic methine carbons (δ_C 103.8, 103.1), six aliphatic α-amino carbons (δ_C 64.4, 62.8, 54.5, 53.6, 46.7, 46.6), and four methylamino carbons (δ_C 31.8, 31.4, 30.9, 30.6). Comparison of the 1D NMR spectra of **1** and echinomycin (**11**) showed significant similarities, except for two terminal olefinic signals (δ_H 6.76, 5.53; 6.79, 5.60; δ_C 134.0, 103.8; 134.0, 103.1) and the absence of two serine resonance in **1**, indicating that two serine residues were replaced by dehydroalanine (Dha) units.

Comprehensive analysis of the ^{1}H–^{1}H COSY (Fig. S12) and HSQC (Fig. S13) of compound **1**, indicated that **1** was comprised of two quinoxalines and eight amino acid moieties (two N-Me-Val, two Ala, two N-Me-Cys, and two Dha) (Fig. 1). The connections between amino acids moieties were confirmed by the HMBC correlations (Fig. S14) from H-2 (δ_H 4.57) of N-Me-Val to C-1 (δ_C 170.7) of N-Me-Cys; from N–CH_3 (δ_H 3.07) of N-Me-Cys to the C-1 (δ_C 172.2) of Ala, and from H-2 (δ_H 5.02) of Ala to C-1(δ_C 163.3) of Dha. Thus, the amino acid sequences were determined as QXA-Dha-Ala-Cys-Val for the upper hemisphere and QXA′-Dha′-Ala′-Cys′-Val′ for the lower hemisphere, based on the interpretation of HMBC correlations (Fig. 4 and S14). Correlations between H-3 (δ_H 4.57) of Cys and C-3 (δ_C 31.5) of Cys′ indicated the presence of a thioacetal linkage connecting the two hemispheres. Accordingly, the HRESIMS/MS fragmentation pattern yields key ions (fragments a–g in Fig. 2) that match the proposed sequence of amino acid residues, thereby strongly supporting the planar structure and the connectivity deduced from HMBC data.

Quinomycin R (**2**) was purified as a yellow amorphous powder. High resolution electrospray ionization mass spectrometry (HRESIMS) data (Fig. S18) revealed a molecular ion at *m/z* 1119.4369 $[M + H]^+$, corresponding to the molecular formula $C_{51}H_{66}N_{12}O_{13}S_2$, indicating 25 degrees of unsaturation. The NMR data of **2** (Table S1, Fig. S21–S23) showed a nearly identical profile to that of **1**, except for the replacement of one Dha unit by a serine residue. Detailed analysis of 2D NMR data (Fig. S24–S28) indicated that the replacement occurred in the upper hemisphere (Fig. S29). Therefore, the structure of compound **2** was established and further confirmed by HRESIMS/MS fragmentation analysis (Fig. S19).

Quinomycin S (**3**) was obtained as a yellow amorphous solid and assigned the molecular formula $C_{51}H_{66}N_{12}O_{13}S_2$ based on

Table 1 ^{1}H (800 MHz) and ^{13}C (201 MHz) NMR data of compound **1** in $CDCl_3$[a]

Pos.	δ_H, mult (*J* in Hz)	δ_C, type	Pos.	δ_H, mult (*J* in Hz)	δ_C, type	Pos.	δ_H, mult (*J* in Hz)	δ_C, type
QXA/QXA′			Ala			Cys′		
2/2′		143.3[a]/143.3[a], C	1		173.1, C	1		170.7, C
3/3′	9.67[a], s/9.67[a], s	143.7[b]/143.7[b], CH	2	5.02, m	46.7, CH	2	5.74, m	53.6, CH
4a/4a′		144.1[c]/144.1[c], C	3	1.45, d (6.8)	18.6, CH_3	3	2.78, d (12.9)	31.5, CH_2
5/5′	8.18[b], m/8.18[b], m	129.6[d]/129.6[d], CH	NH	7.52, d (7.2)			3.32, d (12.4)	
6/6′	7.88[c], m/7.88[c], m	132.1[e]/132.1[e], CH				N–Me	3.02, overlapped	30.6, CH_3
7/7′	7.85[d], m/7.85[d], m	131.2[f]/131.2[f], CH						
8/8′	8.22[e], m/8.22[e], m	130.2[g]/130.2[g], CH						
8a/8a′		140.4[h]/140.4[h], C						
9/9′		162.2/162.2, C						
Dha			Ala′			Val		
1		163.3, C	1		172.6, C	1		169.4, C
2		134.0, C	2	5.02, m	46.6, CH	2	4.79, d (10.4)	64.4, CH
3	5.53, s	103.8, CH_2	3	1.39, d (6.7)	18.7, CH_3	3	2.19, m	27.2, CH
	6.76, s		NH	7.38, d (7.2)		4	1.05, overlapped	20.0, CH_3
NH	10.56, s					5	0.79, d (6.6)	19.0, CH_3
						N–Me	3.07, overlapped	31.8, CH_3
Dha′			Cys			Val′		
1		162.9, C	1		169.4, C	1		170.7, C
2		133.9, C	2	5.66, d (11.1)	54.5, CH	2	4.57, d (11.2)	62.8, CH
3	5.60, s	103.1, CH_2	3	4.57, m	52.6, CH	3	2.26, m	27.3, CH
	6.79, s		S–Me	2.06, s	12.0, CH_3	4	1.05, overlapped	20.0, CH_3
NH	10.58, s		N–Me	3.07, overlapped	30.9, CH_3	5	0.85, d (6.6)	19.4, CH_3
						N–Me	3.07, overlapped	31.4, CH_3

[a] *a–h* assignments for overlapping ^{1}H NMR and ^{13}C NMR resonances with the same superscript may be interchanged.

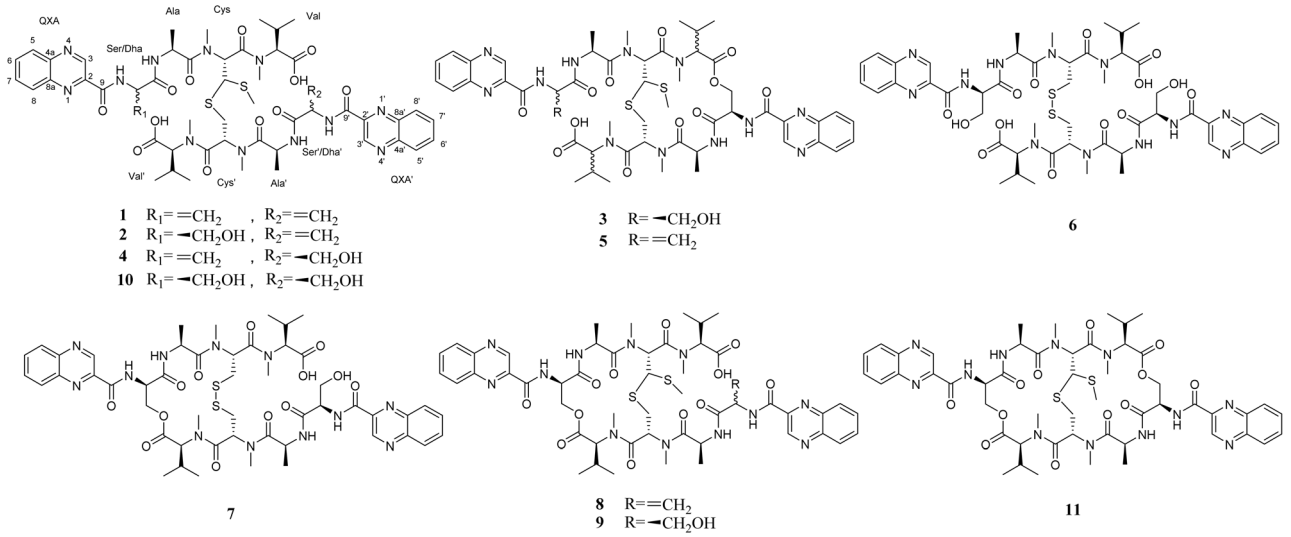

Fig. 1 Structures of compounds **1–11**.

HRESIMS (*m*/*z* 1119.4399 $[M + H]^+$), indicating that is an isomer of **2**. Comprehensive NMR analysis (Table S2, Fig. S33–S40) revealed the absence of one terminal double bond, which was replaced by an ester bond linkage. Comparison of 1D NMR data, suggested that the ester linkage occurred between Val and Ser′, as evidenced by the upfield shift of the β-H in Ser′.

Quinomycin T (**4**) was isolated as a yellow powder with a molecular formula of $C_{51}H_{66}N_{12}O_{13}S_2$, as determined by HRESIMS analysis (*m*/*z* 1119.4364 $[M + H]^+$), indicating that it is an isomer of **2**. However, the NMR spectra of **4** in $CDCl_3$ exhibited poorly resolved and extensively overlapping resonances. Based on literature survey, peptides containing the *N*-methylamino acid residue can exist in solution with multiple conformational isomers due to *cis–trans* isomerization of the amide bond.[12,13] We thus recorded the NMR spectra of **4** at different temperatures in DMSO-d_6, and the signals resolution improved at 53 °C (Fig. 3). According to the ^{1}H NMR (Table S3 and Fig. S45), at least two sets of paired resonances with a 1 : 1

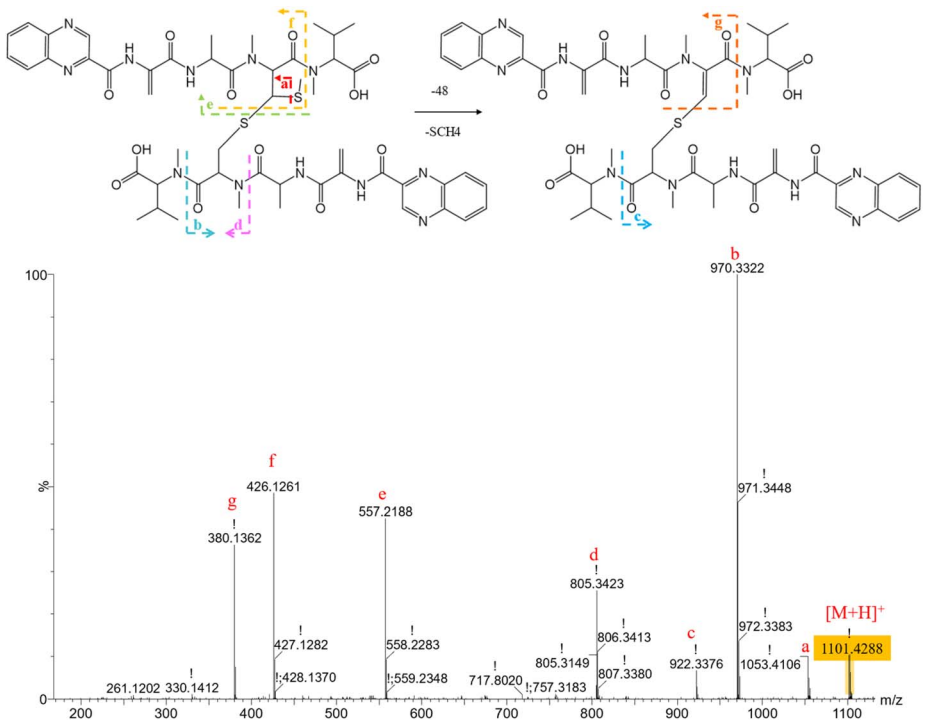

Fig. 2 Selected (+) HRESIMS^2 fragments of compound **1** and MS^2 fragmentation pattern of the protonated molecular ion $[M + H]^+$ (*m*/*z* 1101.4288).

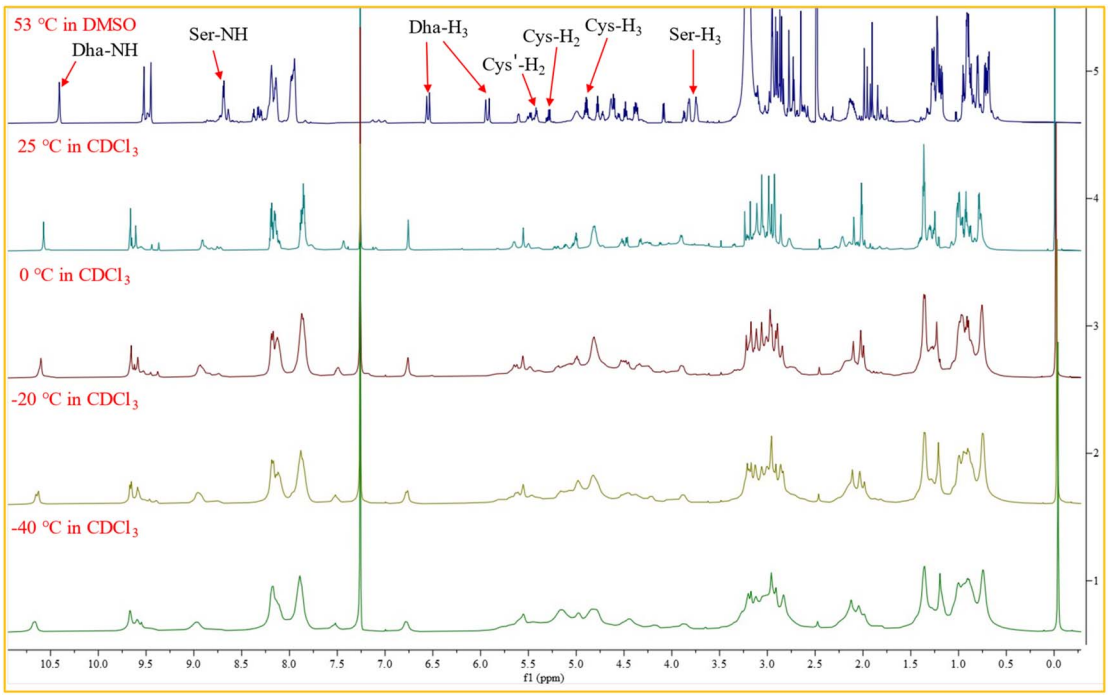

Fig. 3 Effect of temperature on the ^{1}H NMR spectra of compound **4**.

ratio were observed based on the well-resolved terminal olefinic protons, indicating the presence of two conformational isomers. Due to this conformational heterogeneity, the definitive structural assignment for **4** by NMR alone is more challenging than for the other analogues. However, the overall set of data (1D and 2D NMR, together with MS/MS) strongly supports the proposed structure (Fig. 1 and S51). Analysis of the 2D NMR data (Fig. S47–S50) determined that the Dha residue is located in the upper hemisphere, which is the exact opposite of the position in **2**. MS/MS fragmentation analysis provided additional evidence to support this assignment (Fig. S43). The definitive structural assignment for **4** is more challenging due to this conformational heterogeneity, though the combined data (NMR, MS/MS) support the proposed structure.

Quinomycin U (**5**) was obtained as a white amorphous solid. On the basis of HRESIMS studies, the molecular formula $C_{51}H_{64}N_{12}O_{12}S_2$ was deduced at *m*/*z* 1101.4280 $[M + H]^+$. The NMR data (Table S4, Fig. S55 and S56) showed a similar profile to that of **3**, except for the replacement of a serine residue by a Dha unit, indicating the presence of a terminal double bond in the upper hemisphere. Further 2D NMR correlations (Fig. S57–S62) and MS/MS fragmentation (Fig. S53) confirmed this assignment.

Triostin D (**6**) was obtained as a white amorphous powder. It possessed a molecular formula of $C_{50}H_{66}N_{12}O_{14}S_2$ by the HRESIMS ion at *m*/*z* 1123.4348 $[M + H]^+$(calcd for $C_{50}H_{67}N_{12}O_{14}S_2$, 1123.4341). Analysis of the UV and MS/MS spectrum suggested that it was a quinomycin-type octapeptide containing a disulfide cross-link instead of a thioacetal bridge, as inferred from the characteristic neutral loss of the 48 Da observed in **1–5** (Fig. S64). The ^{13}C NMR spectrum (Table S5 and Fig. S67), interpreted with the aid of 2D NMR data (Fig. S70–S74), revealed 26 distinct carbon signals, accounting for only half of the total carbons in the molecular formula and thereby indicating that **6**

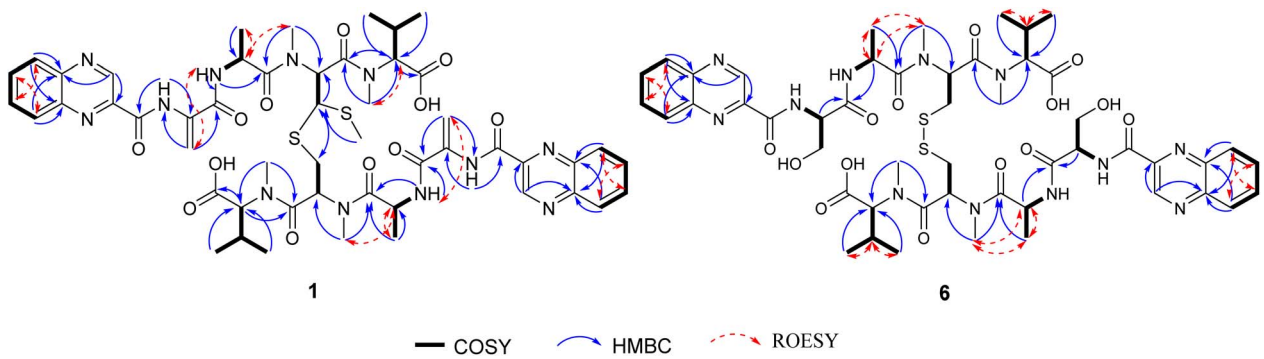

Fig. 4 Key COSY, HMBC, ROESY correlations of representative compounds **1** and **6**.

is a symmetrical dimer. The spectra of **6** were highly similar to those of triostin A[14,15] except for the cleaved ester bonds between Val/Ser′ and Val′/Ser. This structural difference was confirmed by MS/MS fragmentation analysis (Fig. S64) and the absence of the key HMBC correlations for the Val/Ser′ and Val′/Ser ester linkages (Fig. 4 and S75).

Triostin E (**7**) was isolated as a yellow amorphous solid and assigned the molecular formula $C_{50}H_{64}N_{12}O_{13}S_2$ based on HRESIMS data (*m*/*z* 1105.4230 $[M + H]^+$), consistent with the loss of one H_2O unit compared to **6**. The NMR spectra (Table S6, Fig. S79–S81) of compound **7** in $CDCl_3$ also presented severely overlapping resonances due to conformational heterogeneity. Analysis of 2D NMR data (Fig. S82–S86) indicated that the amino acid sequence in **7** were similar to that of **6**, except for an ester bond linkage between Val and Ser′. This was further supported by HRESIMS/MS fragmentation analysis (Fig. S77).

The absolute configurations of the amino acid residues in compounds **1–7** were established by UPLC-MS analysis of their acid hydrolysates derivatized using Marfey's method. Comparison of the FDLA derivatives of the hydrolysates of **1–7** with those of appropriate standard amino acids by UPLC-MS analysis indicated L-, L-, and D-configuration for Ala, N-Me-Val, and Ser, respectively, in compounds **1–4** and **6–7** (Table S7, Fig. S7, S20, S32, S44, S65, and S78). Although compounds **3** and **5** share highly similar structures, both characterized by cleavage of the left-side ester bond, they differ in the stereochemistry of their N-Me-Val residues. Compound **3** contains only the L-configuration, whereas compound **5** comprises both D- and L-forms (Fig. S54). However, the precise stereochemical assignments could not be determined due to the limited sample quantity, which precluded definitive 2D NMR correlation analysis. According to the reported biosynthetic pathway of echinomycin,[16] the formation of disulfide bonds and thioacetal bridges in this class of peptides often occurs as a post-assembly tailoring modification. Therefore, whether the observed stereochemical heterogeneity in compound **5** arises from such post-biosynthetic processes remains unclear and will require further investigation. The configuration of the N-Me-Cys residue was tentatively assigned as L based on the congruence of the ECD spectra (Fig. S4) and optical rotation data between compounds **1–7** and echinomycin (**11**). The absolute configurations of the amino acid residues in compounds **1–7** are summarized in Table S7.

Compounds **1–7** were evaluated for their *in vitro* anti-cancer activity against five human tumor cell lines (K562, HepG2, HT29, DLD-1, NCI-H460) using the MTT method. No significant cytotoxicity (IC_{50} > 10 μM) was observed for compounds **1–7** compared to the positive control cisplatin and compound **11**. In contrast, echinomycin (**11**) exhibited the most potent anti-cancer activity (IC_{50} 0.006 μM). Given this pronounced difference in activity, further IC_{50} determinations were not pursued. To rationalize these biological results, the structural characteristics of **1–7** were further analyzed. Compounds **1–7** shared common structural features: two peptide chains, analogous to those of echinoserine, are connected either by a thioacetal or disulfide bridge alone, or by a sulfur bridge in combination with an ester linkage. The lack of activity in compounds **1–7**, in contrast to the active, fully cyclized echinomycin (**11**), suggests that the integrity of the bicyclic scaffold is likely crucial for biological activity.[8]

Echinomycin, the first discovered natural product bisintercalator, exhibits remarkable antitumor activity and has progressed to phase II clinical trials.[17] Its mechanism of action involves not only bisintercalation into DNA[18,19] but also selective inhibition of hypoxia-inducible factor-1 (HIF-1).[20] However, within this family, structural modifications such as ester bond hydrolysis or sulfoxide formation, while increasing structural diversity, generally lead to a remarkable reduction in bioactivity. In earlier studies, quinomycin analogues with distinct inter-peptide chain linkages have been reported. Some preserve both ester-bond connections without the sulfur cross link,[21] whereas others maintain the sulfur bridge but show cleavage of one or both head-to-tail easter bond.[7,22] These derivatives likewise displayed either undetectable activity or antitumor potency reduced by 2–3 orders of magnitude compared with echinomycin. Earlier study attributed the dramatic decrease in activity to the altered and more flexible conformations resulting from ester bond cleavage, which likely prevent the chromophores from bisintercalating into the duplex DNA effectively.[22] While this explanation is plausible, an alternative possibility is that the presence of free carboxylic acid groups reduces membrane permeability and consequently limits cellular uptake.

To distinguish between these two hypotheses, we designed and performed the following experiments. Two structurally distinct compounds, **10** and **11**, were selected and administered to NCI-H460 cells at different concentrations. Cells were harvested at various time points post-treatment, and the intracellular and extracellular levels of both compounds were analyzed by UPLC-HRMS. The results demonstrated that the active compound **11** was readily detectable inside the cells at multiple time points, with particularly prominent accumulation observed at 24 h, coinciding with the onset of apoptosis (Fig. S93A). In contrast, compound **10** was not detected intracellularly and was only present in the culture medium. This intriguing observation prompted further mechanistic speculation. Cells possess intrinsic protective systems capable of expelling xenobiotics through efflux transporters such as P-glycoprotein (P-gp) and multidrug resistance-associated protein 1 (MPR1).[23] Given that **11** induced apoptosis, intracellular ATP levels are likely to decline following treatment. In the absence of sufficient energy supply, ATP-dependent efflux pumps may become functionally impaired, leading to intracellular accumulation of **11**. The observed dose-dependent intracellular levels of **11** further supports this interpretation (Fig. S93B). In contrast, compound **10** was undetectable within the cells, which may be attributed to its poor membrane permeability and/or efficient ATP-dependent efflux, thereby resulting in intracellular concentrations below the detection limit of mass spectrometry.

To further evaluate this hypothesis, we performed another experiment. An LC-MS method was employed to examine the distribution of compounds **10** and **11** in the producing strain after fermentation. The results revealed that compound **11** was present in both the mycelia and the culture broth. In contrast,

compound **10** was predominantly detected in the broth, with only trace amounts observed in the mycelia (Fig. S94). These findings suggest that ester-bond-cleavaged derivatives such as **1–10** may represent naturally occurring metabolites with low-toxicity, and generated by the producing strain as part of a self-resistance mechanism.[24] These compounds may exhibit reduced membrane permeability, and even if small amounts enter the cells, they could be efficiently eliminated by ATP-driven efflux transporters.

Experimental section

General experimental procedures

High-resolution electrospray ionization mass spectrometry (HRESIMS) and MS/MS data were acquired using a Waters Xevo G2 Q-T of instrument equipped with a Waters ACQUITY UPLC BEH C18 column (100 × 2.1 mm, 1.7 μm). NMR spectra were acquired using Bruker AVANCE III HD 500 MHz and Ascend TM 800 MHz NMR spectrometers. Optical rotations and ECD spectra were acquired using a JASCO J-1500 spectropolarimeter (JASCO, Tokyo, Japan). Semipreparative HPLC was performed on an LC2030 system (Shimadzu, Kyoto, Japan) equipped with a DAD detector, using a Sunniest PFP&C18 column (10 × 250 mm, 5 μm) at a flow rate of 2.0 mL min^{-1}.

Extraction and separation of crude extracts

The *Streptomyces* sp. GXIMD 03507 was isolated from mangrove rhizosphere soil in Dongxing, Guangxi, China. Genomic DNA extraction, PCR amplification, and sequencing were carried out by Shanghai BIOZERON Biotech. Co., Ltd. The partial 16S rRNA gene fragment was amplified using the universal primers 27F (5′-AGAGTTTGATCCTGGCTCAG-3) and 1492R (5′-TACGGCTACCTTGTTACGACTT-3′). Strain identification was based on morphological characteristics and 16S rRNA gene sequence analysis, and the sequence has been deposited in GenBank under the accession number PX472909 (Fig. S1). The strain is preserved at the Institute of Marine Drugs, Guangxi University of Chinese Medicine, Nanning, People's Republic of China.

The strain was initially grown and maintained on an agar plate with 38# medium (glucose 4 g L^{-1}, yeast extract 4 g L^{-1}, malt extract 10 g L^{-1}, agar 20 g L^{-1}, multivitamin 500 μl L^{-1}, marine salt 15 g L^{-1}, distilled water 1 L, pH = 7.2–7.4) at 28 °C for 4 days to produce spore suspension. The spores were inoculated into 1000 mL Erlenmeyer flasks containing 200 mL of 38# medium at 28 °C, 200 rpm for 7 days. The culture broth (60 L) was centrifuged (4300 rpm, 30 min), and the resulting supernatant was subjected to microporous resin (Amberlite XAD16, 20–60 mesh) adsorption, followed by multiple elution with methanol, and then partitioned against ethyl acetate to obtain the crude organic extract (10.79 g). The extract was subjected to Vacuum Liquid Chromatography (VLC) on silica gel (200–300 mesh) eluted with CH_2Cl_2–MeOH (1 : 0, 50 : 1, 25 : 1, 20 : 1, 15 : 1, 10 : 1, 5 : 1, 3 : 1, 0 : 1, v/v) to obtain thirteen fractions (Fr.1–Fr.13). Based on HPLC-PDA-MS analysis, Fr.5 (1.45 g), Fr.7 (584.9 mg), Fr.9 (396.3 mg) and Fr.10 (1.02 g), which were tentatively identified as containing quinomycin-type compounds (exhibiting maximum absorption at 201, 242, 318, and 324 nm, similar to echinomycin), were further fractionated on Sephadex LH-20 using CH_2Cl_2/MeOH (1 : 1, v/v), respectively. Fr.5.2 (463.9 mg) was separated by semipreparative HPLC (75% aqueous MeOH with 0.1% formic acid) to obtain compound **3** (t_R = 20.6 min, 18 mg) (Fig. S90), and by semipreparative HPLC (52% aqueous MeCN with 0.1% formic acid) to obtain compound **5** (t_R = 41.6 min, 4.7 mg) (Fig. S91). Fr.7.1 (143.8 mg) was separated by semipreparative HPLC (50% aqueous MeCN with 0.1% formic acid) to obtain compound **1** (t_R = 45.7 min, 7.6 mg), compound **7** (t_R = 11.7 min, 12.3 mg) (Fig. S88). Fr.9.1 (396.3 mg) was separated by semipreparative HPLC (44% aqueous MeCN with 0.1% formic acid) to obtain compound **2** (t_R = 26.4 min, 36.1 mg), compound **4** (t_R = 28.7 min, 10.1 mg) (Fig. S89). Fr.10.1 (597.4 mg) was separated by semipreparative HPLC (37% aqueous MeCN with 0.1% formic acid) to obtain compound **6** (t_R = 23.1 min, 5 mg) (Fig. S92).

Quinomycin Q (**1**). White amorphous solid; $[\alpha]_D^{20}$ −110.1 (*c* 0.25, MeOH); NMR data, Table 1 and Fig. S8–S16; HRESIMS *m*/*z* 1101.4288 $[M + H]^+$ (calcd for $C_{51}H_{65}N_{12}O_{12}S_2$, 1101.4286, Δ 0.18 ppm).

Quinomycin R (**2**). Yellow amorphous solid; $[\alpha]_D^{20}$ −122.1 (*c* 0.25, MeOH); NMR data, Table S1 and Fig. S21–S28; HRESIMS *m*/*z* 1119.4369 $[M + H]^+$ (calcd for $C_{51}H_{67}N_{12}O_{13}S_2$, 1119.4392, Δ 2.05 ppm).

Quinomycin S (**3**). Yellow amorphous solid; $[\alpha]_D^{20}$ −162.1 (*c* 0.25, MeOH); NMR data, Table S2 and Fig. S33–S40; HRESIMS *m*/*z* 1119.4399 $[M + H]^+$ (calcd for $C_{51}H_{67}N_{12}O_{13}S_2$, 1119.4392, Δ 0.63 ppm).

Quinomycin T (**4**). Yellow amorphous solid; $[\alpha]_D^{20}$ −76.0 (*c* 0.25, MeOH); NMR data, Table S3 and Fig. S45–S50; HRESIMS *m*/*z* 1119.4364 $[M + H]^+$ (calcd for $C_{51}H_{67}N_{12}O_{13}S_2$, 1119.4392, Δ 2.5 ppm).

Quinomycin U (**5**). White amorphous solid; $[\alpha]_D^{20}$ −82.1 (*c* 0.25, MeOH); NMR data, Table S4 and Fig. S55–S61; HRESIMS *m*/*z* 1101.4280 $[M + H]^+$ (calcd for $C_{51}H_{65}N_{12}O_{12}S_2$, 1101.4286, Δ 0.54 ppm).

Triostin D (**6**). White amorphous solid; $[\alpha]_D^{20}$ −226.2 (*c* 0.25, MeOH); NMR data, Table S5 and Fig. S66–S74; HRESIMS *m*/*z* 1123.4348 $[M + H]^+$ (calcd for $C_{50}H_{67}N_{12}O_{14}S_2$, 1123.4341, Δ 0.62 ppm).

Triostin E (**7**). Yellow amorphous solid; $[\alpha]_D^{20}$ −152.1 (*c* 0.25, MeOH); NMR data, Table S6 and Fig. S79–S86; HRESIMS *m*/*z* 1105.4230 $[M + H]^+$ (calcd for $C_{50}H_{65}N_{12}O_{13}S_2$, 1105.4235, Δ 0.45 ppm).

Marfey's analysis

Analysis was carried out following the published method.[25] Compounds **1–7** (100 μg) were dissolved in 6 N HCl (100 μL), and heated at 110 °C for 24 h. After cooling to room temperature, the hydrolysates were dried under reduced pressure. The hydrolysates were treated with 1 M $NaHCO_3$ (40 μL) and then reacted with (5-fluoro-2,4-dinitrophenyl-L-leucineamide, 1% solution in acetone, 100 μL) L-FDLA at 40 °C for 1 h. After cooling to room temperature, the mixture was added with 1 M HCl (25 μL) to neutralize and terminate the reaction. MeOH was

then added to the quenched reaction to afford a total volume of 1 mL, and filtered (0.25 μm PTFE) before subjected to HPLC-HRMS analysis (Waters ACQUITY UPLC BEH C18 column 100 × 2.1 mm i.d.; 1.7 μm, 0.3 mL min^{-1}) with linear gradient elution (20–50% solvent Bin 10 min; solvent A: H_2O with 0.1% formic acid, solvent B: 100% MeCN).

ECD analysis

The circular dichroism experiment was performed on a Jasco J-1500 CD spectrophotometer utilizing a 1 mm cuvette. Compounds **1–7** dissolved in MeOH solution were made up as 0.25 mg mL^{-1} solutions. The spectra were recorded from 400 to 200 nm with 100 nm min^{-1} scanning speed at the response time of 1 s and 2 nm bandwidth.

Anti-tumor assay

The anti-tumor activities of compounds **1–11** against 5 tumor cell lines including: human chronic myelogenous leukemia cell line (k562), human hepatoma cell line (HepG2), human colorectal cancer cell lines (HT29, DLD-1), human non-small cell lung carcinoma cell line (NCI-H460) were determined by MTT method.[26] All cell lines were purchased from Zhongqiao Xinzhou Biotechnology Co., Ltd, Shanghai.

MTT assay: briefly, logarithmic cells were digested with 0.25% pancreatic enzyme-EDTA and plated in the 96-well plates at a concentration of 2000–3000/100 μL per well, incubated in either RPMI-1640 medium (for K562, HT-29, DLD-1 and NCI-H460) or DMEM medium (for HepG2) at 37 °C in a humidified atmosphere containing 5% CO_2 for 24 h. After this incubation, compounds **1–11** P were added in triplicate at final concentrations of 0.006–10 μM. The cells were incubated further at 37 °C for 96 h, the medium was removed, and 200 μL MTT of 0.5 mg mL^{-1} in medium was added. After 4 h incubation, the medium was removed, and 200 μL DMSO was added to dissolve the formazan crystals. Absorbance was measured at a wavelength of 560 nm with background subtraction at 650 nm. The dose–response curves were generated with Sigma Plot and IC_{50} values were determined.

Determination of compounds 10 and 11 in NCI-H460 cells

NCI-H460 cells were seeded into 6-well plates at a density of 4 × 10^5 cells per well and cultured for 24 h. Cells were then treated with fresh medium containing the indicated concentrations of compounds **10** and **11** (2.5, 5, 10, and 20 μM). After incubation at 37 °C for 0.5, 1, 3, 6, 12 and 24 h, the medium was collected and processed separately later, and the cells were washed twice with 2 mL PBS with 0.1% serum. Following trypsin digestion, cells were harvested by centrifugation (1000 rpm, 3 min). The cell pellet was resuspended in 100 μL of PBS, followed by the addition of approximately 1 mL of cell lysis buffer and vortexing. Both the cell lysates and the collected culture medium were extracted with ethyl acetate and concentrated under reduced pressure, respectively. The resulting residues were each reconstituted in methanol to a final volume of 1 mL, and the supernatant was subsequently analyzed by HPLC-HRMS.

Determination of the distribution of compounds 10 and 11 in the fermentation broth and mycelia

The strain was initially cultivated in 0.2 L 38# medium. After 7 days of fermentation, the culture broth was centrifuged to separate the mycelia from the supernatant. The supernatant was adsorbed onto microporous resin (Amberlite XAD16, 20–60 mesh), eluted repeatedly with methanol, and subsequently partitioned with ethyl acetate to afford the crude broth extract. The mycelial pellet was washed three times with distilled water, extracted with methanol under ultrasonication, and centrifuged (4300 rpm, 30 min). The methanol solution was concentrated *in vacuo* and partitioned with ethyl acetate to yield the crude mycelial extract. Both extracts were subsequently analyzed by HPLC-HRMS.

Conclusions

This study reports the isolation and characterization of seven novel quinomycin-type octapeptides from the mangrove rhizosphere-derived *Streptomyces* sp. GXIMD 03507 through an LC-PDA-MS guided chemical investigation. These compounds were characterized by the cleavage of one or both ester bonds. Their planar structures and absolute configurations were elucidated by detailed NMR, $ESIMS^2$ fragments, advanced Marfey's method and ECD analyses. Compounds **1–7** exhibited poor antitumor activity (IC_{50} > 10 μM), which may be associated with their structural differences from echinomycin (**11**), paritcularly the two head-to-tail ester bonds. These structural alterations may lead to reduced membrane permeability and/or enhanced susceptibility to ATP-dependent efflux mechanism, thereby limiting intracellular accumulation and consequently diminishing their biological activity. This study expands the chemical diversity of quinomycin-type peptides and reinforces the stringent structural requirements for biological activity within this family, providing valuable insights for future analogue design and biosynthetic engineering.

Author contributions

Conceptualization, X. L. and X. J.; methodology, Y. W., X. L. and X. J.; software, Z. T., P. X. and M. Z.; validation, X. L.; formal analysis, M. Z., Y. W., Z. T. and X. L.; investigation, R. Q., Q. J., Y. D., C. C. and Z. T.; resources, X. L.; data curation, M. Z., Y. W., Z. T. and X. L.; writing – original draft preparation, Y. W., X. L. and X. J.; writing – review and editing, Y. W., X. L. and X. J.; visualization, X. L.; supervision, X. L. and X. J.; project administration, Y. L., X. J. and X. L.; funding acquisition, Y. L., X. J. and X. L. All authors have read and agreed to the published version of the manuscript.

Conflicts of interest

There are no conflicts to declare.

Data availability

The supporting data has been provided as part of the supplementary information (SI). Supplementary information: Tables S1–S6: the ^{1}H and ^{13}C NMR data of **2–7**; Table S7: the amino acids configurations of **1–7**; Fig. S1: phylogram generated by the concatenation of the GXIMD 03507 of the *Streptomyces* sp.; Fig. S2 and S3: LC-PDA-MS and UV spectra of crude extract; Fig. S4–S92: the ESI-MS^2, NMR, Marfey's analysis, CD and Key COSY, HMBC, ROESY/NOESY correlations spectrum of compounds **1–7**; Fig. S93: LC-MS analysis of the intracellular distribution of compound **11**. Fig. S94: LC-MS determination of compounds **10** and **11** in the fermentation broth and mycelium. See DOI: https://doi.org/10.1039/d5ra09728b.

Acknowledgements

This research was supported by the National Natural Science Foundation of China (82560684), Natural Science Foundation of Guangxi (2023GXNSFBA026139), Joint fund project for regional innovation and development set up by National Natural Science Foundation (U24A20808), the National Natural Science Foundation of China (82160669), Natural Science Foundation of Guangxi (AD22035167), Guangxi Special Support Program for Maritime Economic Talent Cultivation (2025XHRC27), and Innovation Project of Guangxi Graduate Education (YCSY2025100).

Notes and references

1 J. Sui, X. He, G. Yi, L. Zhou, S. Liu, Q. Chen, X. Xiao and J. Wu, *PeerJ*, 2023, **11**, e16156.
2 M.-J. Wu, B. Xu and Y.-W. Guo, *Mar. Drugs*, 2022, **20**, 535.
3 W. Lin, G. Li and J. Xu, *Mar. Drugs*, 2023, **21**, 239.
4 D.-B. Xu, W.-W. Ye, Y. Han, Z.-X. Deng and K. Hong, *Mar. Drugs*, 2014, **12**, 2590–2613.
5 S. Dharmaraj, *World J. Microbiol. Biotechnol.*, 2010, **26**, 2123–2139.
6 X. Shi, *Nat. Prod. Rep.*, 2025, **42**, 1091–1119.
7 Z. Xin, G. Ting, L. Fu, Z. Pei-Cheng, Z. Wan-Qi, L. Yan and Z. Ping, *Mar. Drugs*, 2015, **13**, 6947–6961.
8 A. M. Socha, K. L. LaPlante, D. J. Russell and D. C. Rowley, *Bioorg. Med. Chem. Lett.*, 2009, **19**, 1504–1507.
9 S. Blum, H.-P. Fiedler, I. Groth, C. Kempter, H. Stephan, G. Nicholson, J. W. Metzger and G. Jung, *J. Antibiot.*, 1995, **48**, 619–625.
10 A. Dell, D. H. Williams, H. R. Morris, G. A. Smith, J. Feeney and G. C. K. Roberts, *J. Am. Chem. Soc.*, 1975, **97**(9), 2497–2502.
11 Z. Yang, L. Shao, M. Wang, M. Rao, M. Ge and Y. Xu, *J. Antibiot.*, 2019, **72**, 164–168.
12 D. Pal and P. Chakrabarti, *J. Mol. Biol.*, 1999, **294**, 271–288.
13 A. B. Mauger, W. J. Rzeszotarski and R. A. Ford, *Org. Magn. Reson.*, 1973, **5**, 231–234.
14 K. Hattori, K. Koike, K. Okuda, T. Hirayama, M. Ebihara, M. Takenaka and H. Nagasawa, *Org. Biomol. Chem.*, 2016, **14**, 2090–2111.
15 H. Otsuka, J. Shoji, K. Kawano and Y. Kyogoku, *J. Antibiot.*, 1976, **29**, 107–110.
16 M. Sato, T. Nakazawa, Y. Tsunematsu, K. Hotta and K. Watanabe, *Curr. Opin. Chem. Biol.*, 2013, **17**, 537–545.
17 W. J. Gradishar, N. J. Vogelzang, L. J. Kilton, S. J. Leibach, A. W. Rademaker, S. French and Al. B. Benson, *Invest. New Drugs*, 1995, **13**, 171–174.
18 C. L. Mazzitelli, Y. Chu, J. J. Reczek, B. L. Iverson and J. S. Brodbelt, *J. Am. Soc. Mass Spectrom.*, 2007, **18**, 311–321.
19 B. D. Rackham, L. A. Howell, A. N. Round and M. Searcey, *Org. Biomol. Chem.*, 2013, **11**, 8340.
20 D. Kong, E. J. Park, A. G. Stephen, M. Calvani, J. H. Cardellina, A. Monks, R. J. Fisher, R. H. Shoemaker and G. Melillo, *Cancer Res.*, 2005, **65**, 9047–9055.
21 Q. Lu, G. Wu, X. Hao, X. Hu, H. Cai, X. Liu, X. You, H. Guo and C. Sun, *Mar. Drugs*, 2023, **21**, 143.
22 A. Wang, S. Li, Y. Wei, G. Wang, W. Shi, Y. Shang, L. Yu, S. Chen, Y. Li and M. Gan, *J. Antibiot.*, 2024, **77**(8), 506–514.
23 S. Mirzaei, M. H. Gholami, F. Hashemi, A. Zabolian, M. V. Farahani, K. Hushmandi, A. Zarrabi, A. Goldman, M. Ashrafizadeh and G. Orive, *Drug Discov. Today*, 2022, **27**, 436–455.
24 X. Shi, *Nat. Prod. Rep.*, 2025, **42**, 1091–1119.
25 X. Lin, Z. Tang, Y. Gan, Z. Li, X. Luo, C. Gao, L. Zhao, L. Chai and Y. Liu, *J. Nat. Prod.*, 2023, **86**, 994–1002.
26 N. P. Ariantari, E. Ancheeva, M. Frank, F. Stuhldreier, D. Meier, Y. Gröner, I. Reimche, N. Teusch, S. Wesselborg, W. E. G. Müller, R. Kalscheuer, Z. Liu and P. Proksch, *RSC Adv.*, 2020, **10**, 7232–7240.